Transferrin receptor 2 deficiency promotes macrophage polarization and inflammatory arthritis

Maria G. Ledesma-Colunga [a], Ulrike Baschant [a], Heike Weidner [a], Tiago C. Alves [b], Peter Mirtschink [b], Lorenz C. Hofbauer [a], Martina Rauner [a,*]

[a] *Department of Medicine III and Center for Healthy Aging, Technische Universität Dresden, Dresden, Germany*
[b] *Institute of Clinical Chemistry and Laboratory Medicine, Technische Universität Dresden, Dresden, Germany*

A B S T R A C T

Objective: Rheumatoid arthritis is an inflammatory joint disease in which synovial iron deposition has been described. Transferrin receptor 2 (Tfr2) represents a critical regulator of systemic iron levels. Loss of Tfr2 function in humans and mice results in iron overload. As iron contributes to inflammatory processes, we investigated whether Tfr2-deletion affects the pathogenesis of inflammatory arthritis in an iron-dependent manner.
Methods: Using a global and conditional genetic disruption of *Tfr2,* we assessed the relevance of Tfr2 in K/BxN serum-transfer arthritis (STA) and macrophage polarization.
Results: Male $Tfr2^{-/-}$ mice subjected to STA developed pronounced joint swelling, and bone erosion as compared to $Tfr2^{+/+}$ littermate-controls ($P < 0.01$). Furthermore, an increase of neutrophils and macrophages/monocytes was observed in the inflammatory infiltrate within the paws of $Tfr2^{-/-}$ mice. To elucidate whether Tfr2 in myeloid cells has a direct role in the pathogenesis of arthritis or whether the effects were mediated via the systemic iron overload, we induced STA in $Tfr2^{fl/fl}$-*LysMCre* + mice, which showed normal iron-loading. *Cre* + female mice displayed increased disease development compared to *Cre*-controls. As macrophages regulate iron availability and innate immunity, we hypothesized that Tfr2-deficiency would polarize macrophages toward a pro-inflammatory state (M1) that contributes to arthritis progression. In response to IFN-γ stimulation, $Tfr2^{-/-}$ macrophages showed increased expression of M1-like cytokines, IFN-γ-target genes, nitric-oxide production, and prolonged STAT1 activation compared to $Tfr2^{+/+}$ macrophages ($P < 0.01$), while pre-treatment with ruxolitinib abolished Tfr2-driven M1-like polarization.
Conclusion: Taken together, these findings suggest a protective role of Tfr2 in macrophages on the progression of arthritis via suppression of M1-like polarization.

1. Introduction

Rheumatoid arthritis (RA) is an autoimmune disease characterized by tissue inflammation, synovial proliferation, and the destruction of cartilage and bone. While the initial triggers of the disease remain unknown, it is widely recognized that hyperplasia results from leukocytes infiltrating the rheumatoid synovium and the overproduction of a large number of cytokines including TNFα, IL-6, IL-1, and IL-17 [1]. The interplay between synoviocytes with cells from the innate and adaptive immune system (neutrophils, monocytes, and macrophages as well as T lymphocytes and B cells) ruled by pro-inflammatory cytokines, perpetuates the inflammatory cascade and promotes matrix destruction via skeletal cells, eventually causing cartilage erosion and bone loss [2,3]. Even though RA mainly affects peripheral synovial joints, it is also a systemic disease that is frequently accompanied by anemia, characterized by low serum iron concentrations and high ferritin levels. Intriguingly, despite lower iron serum concentrations, patients with RA demonstrate higher concentrations of free iron in the synovial fluid as well as increased iron depositions in the synovial membrane relative to those without RA [4]. These iron depositions are presumed to derive predominantly from intra-articular hemorrhages and an increase in uptake of iron into synovial cells and macrophages, mainly raised by pro-inflammatory cytokines. The latter in turn perpetuates inflammation by aiding in the production of free oxygen radicals (ROS) [5]. Furthermore, early clinical studies have demonstrated negative clinical outcomes in patients with RA receiving iron supplementation for the treatment of anemia [6]. Similarly, intravenous iron infusions in arthritic rats worsen synovial inflammation and enhance disease severity [7,8], while treatment with deferoxamine, an iron chelator, reduces the incidence and severity of joint inflammation [9].

As an essential element for life, iron homeostasis is tightly controlled to ensure that the proper amount is present and that excess is stored in non-toxic forms [10]. Efflux of iron into plasma from enterocytes, macrophages, and hepatocytes is under the control of the iron-regulator

hepcidin, secreted by hepatocytes. Hepcidin binds to its receptor ferroportin, the sole iron exporter, and controls its activity through internalization and degradation, or occlusion [11,12]. Disease-causing mutations in the main upstream receptors required for its activation, TFR2 (transferrin receptor 2), the hemochromatosis protein HFE, and the BMP co-receptor HJV (hemojuvelin) cause hereditary hemochromatosis, a disorder of iron overload with low hepcidin levels [13]. TFR2 is expressed predominately in the liver and erythrocyte compartment [14], although recent reports also demonstrated its expression in macrophages [15], osteoblasts [16], and neurons [17]. Loss of TFR2 function in humans and mice results in systemic iron overload, which is mainly deposited in the liver and other parenchymal organs [18]. Apart from its hepatic iron-regulatory function, TFR2 is a crucial component of the erythropoietin receptor (EPOR) complex and is required for efficient erythropoiesis [19]. Moreover, TFR2 modulates BMP and Wnt signaling, thereby, controlling bone mass maintenance via direct actions in osteoblasts [16], placing this iron sensor at the crossroads of iron homeostasis, red cell production, and bone turnover. As iron has a critical role in mounting effective immune responses and TFR2 plays a critical role in controlling systemic iron availability, erythropoiesis, and bone homeostasis, we hypothesized that Tfr2 and/or iron overload play a major role in the development and progression of chronic inflammation such as RA.

2. Materials and methods

Materials and methods are available in a supplemented information file.

3. Results

3.1. Tfr2-deficient mice develop more severe arthritis

Tfr2 mRNA and protein expression were investigated in inflamed arthritic paws and were found to be significantly upregulated. In addition, immunohistochemistry showed that Tfr2 expression co-localized with F4/80 expression, suggesting that macrophages in the bone marrow and synovium express Tfr2 (Fig. S1A). Based on this observation, we further explored whether Tfr2 is involved in arthritis development and progression by subjecting *Tfr2*-deficient and sufficient male and female mice to K/BxN serum-transfer arthritis (STA) [20]. Consistently with previous reports, $Tfr2^{-/-}$ mice are iron overloaded. $Tfr2^{-/-}$ male mice showed increased liver iron content and transferrin saturation, with low mRNA expression of *Hamp* compared to $Tfr2^{+/+}$ mice (Table S2). STA was significantly more pronounced in iron overloaded *Tfr2*-deficient ($Tfr2^{-/-}$) male mice showed higher arthritic clinical scores than those of wild-type littermate control ($Tfr2^{+/+}$) on days 6, 8, and 10 (Fig. 1A). Furthermore, joint swelling, which peaked at day 7 post-STA (Fig. 1B), indicated higher disease severity in *Tfr2*-deficient mice. Histological analysis using H&E staining showed that synovitis of tibiotalar joints was more severe in male $Tfr2^{-/-}$ mice than in $Tfr2^{+/+}$ mice. On day 10 post-STA, $Tfr2^{-/-}$ male mice showed marked cellular infiltration mixed with multiple layered synovial lining cells and hyperplasia compare to arthritic $Tfr2^{+/+}$ mice (Fig. 1C). mRNA expression of inflammatory molecules involved in arthritis progression including *Il1b, Il6, Ifng, Nos2,* and the chemokine receptors *Cxcr2* and *Cxcr4* was significantly upregulated in paw extracts from male $Tfr2^{-/-}$ mice compared with $Tfr2^{+/+}$ mice (Fig. 1D). Interestingly, in spite of iron overload (Table S2), $Tfr2^{-/-}$ female mice displayed similar arthritis scores, synovial inflammation, and mRNA expression of inflammatory markers compared to $Tfr2^{+/+}$ female mice (Fig. S2), suggesting a sexual dimorphism in which $Tfr2^{-/-}$ male mice have more severe arthritis than females.

In patients with RA, increased levels of pro-inflammatory cytokines in the synovial fluid and serum play a pivotal role in the pathogenesis of the disease [21]. To analyze Tfr2 involvement in systemic inflammation, we measured the levels of several inflammatory proteins in the serum of $Tfr2^{+/+}$ and $Tfr2^{-/-}$ male mice (Fig. 1E, Table S3). Levels of cytokines and chemokines IL-7, IL-16, IL-17, IL-27, TNFα, CXCL1, CCL2, CXCL11, and CXCL13, as well as biomarkers of inflammation, such as sCAM-1, G-CSF, M-CSF, TIMP-1, and TREM-1, were significantly up-regulated in male $Tfr2^{-/-}$ mice, suggesting a robust inflammation in arthritic *Tfr2*-deficient mice.

Oxidative stress plays a crucial role in the pathogenesis of RA [22], and iron overload predisposes to reactive oxygen species (ROS) production and tissue injury [23]. To analyze the participation of *Tfr2*-deficiency mediated systemic iron overload and the induction of oxidative stress, we determined the iron content and the mRNA expression of distinctive enzymatic antioxidant systems in paw extracts from $Tfr2^{-/-}$ and $Tfr2^{+/+}$ mice. Total iron content in the tibiotalar joint was significantly upregulated in $Tfr2^{-/-}$ compared to $Tfr2^{+/+}$ mice under STA conditions (Fig. S3A). Notwithstanding, iron accumulation, mRNA levels of *Nrf2* and *Nrf2*-mediated response genes to oxidative stress (*Hmox1, Nqo1, Txn2*) (Figs. S3B and C), and other antioxidant-system genes including *Sod2*, *Cat*, and *Gpx4* were unchanged (Fig. S3C). Although the expression of *Gsr1* and *Gsta1* was significantly upregulated in STA joints from $Tfr2^{-/-}$ mice (Fig. S3C), the data collectively suggest that the increased susceptibility of $Tfr2^{-/-}$ to arthritis progression may result independently of joint iron accumulation and oxidative stress.

Moreover, RA is a systemic disease and in addition to the joints, liver is a major target of oxidative stress [24]. Based on this notion, we sought to determine the oxidative status of this organ in $Tfr2^{-/-}$ and $Tfr2^{+/+}$ under healthy and arthritic conditions. mRNA expression levels of *Nrf2, Gsta1*, *Txn2* and *Sod2* (Figs. S3D and E) were significantly upregulated in the liver from healthy $Tfr2^{-/-}$ mice compared to $Tfr2^{+/+}$ mice, and diminished in STA conditions, while *Gsr* and *Cat* expression were only impaired in STA $Tfr2^{+/+}$ and $Tfr2^{-/-}$ mice, respectively (Fig. S3E). mRNA levels of *Hmox1*, *Nqo1*, and *Gpx4* in STA mice from both genotypes were not different compared to those found in control healthy mice (Figs. S3D and E).

Early hallmarks of inflammatory disease in RA are articular and systemic bone erosions [25]. To address the participation of Tfr2 in bone loss during arthritis we assessed the expression of osteoclast marker genes on day 10 post-STA when the chronic phase had been reached. Paw lysates from $Tfr2^{-/-}$ male mice showed increased mRNA expression of *Acp5* and *Ctsk* compared to $Tfr2^{+/+}$ mice (Fig. 2A). In addition, micro-CT imaging of bone surfaces in the ankles showed higher bone erosion scores (Fig. 2B), a significant increase in the number of TRAP-positive cells (osteoclast number), and a larger area of inflamed synovium in $Tfr2^{-/-}$ mice (Fig. 2C). Furthermore, we determined serum levels of TRAcP5b and P1NP, as readouts of systemic bone turnover *in vivo,* and bone mass in the axial skeleton. In line with our previous findings [16], increased TRAcP5b and P1NP levels were detected in the serum of $Tfr2^{-/-}$ mice, compared to $Tfr2^{+/+}$ mice (Fig. 2D). Furthermore, although the bone mineral density did not differ between $Tfr2^{-/-}$ and $Tfr2^{+/+}$ STA mice, bone loss in STA mice was significantly higher in $Tfr2^{-/-}$ (6.8%) than in $Tfr2^{+/+}$ (4.15%) compared with their healthy control mice (Fig. 2E). Collectively, these results suggest that loss of *Tfr2* increases osteoclasts activity and local as well as systemic bone erosion in inflammatory arthritis.

3.2. Constitutive lack of Tfr2 is associated with extensive recruitment of neutrophils and macrophages into arthritic joints

Orchestration of neutrophil and macrophage recruitment is a crucial step in the pathogenesis of arthritis [20]. To further investigate whether *Tfr2*-deficiency participates in cell recruitment and their influx into the joints in STA, we analyzed the frequency of hematopoietic cells and myeloid progenitors (neutrophils and macrophage/monocytes) in the inflammatory infiltrate within the paws at the disease maximum (day 7 post-STA) (Fig. 3A). Consistent with the histological observations, the fraction of infiltrating hematopoietic cells (CD45$^+$), in particular, myeloid precursors (CD45$^+$CD11b$^+$) was increased in $Tfr2^{-/-}$ mice
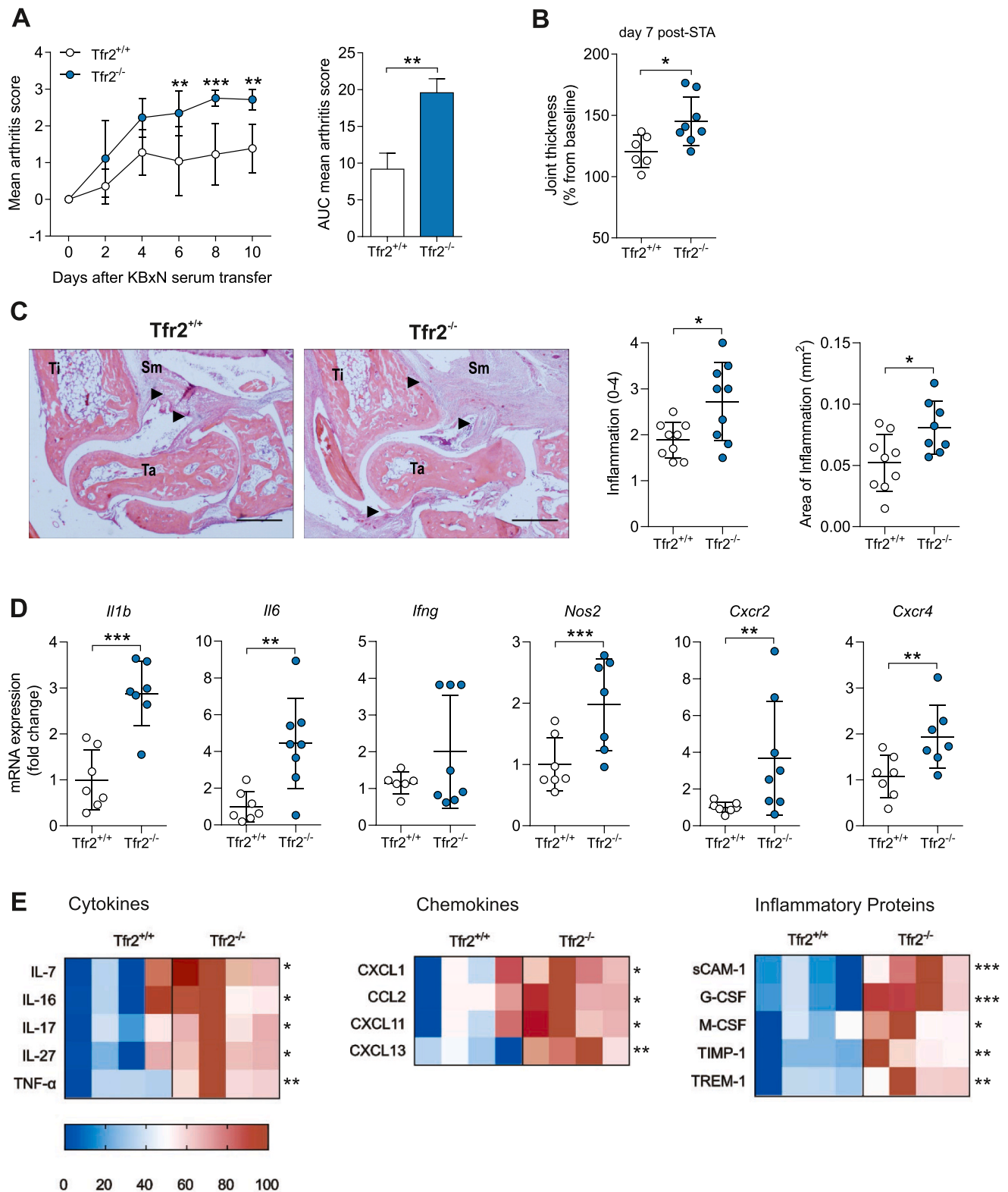
Fig. 1. Global *Tfr2*-deletion enhances arthritis severity.
(A) Arthritis progression assessed by mean clinical scores of $Tfr2^{+/+}$ (n = 9, white symbols) and $Tfr2^{-/-}$ (n = 9, blue symbols) in male mice challenged with K/BxN serum-transfer arthritis (STA), and area under the curve (AUC). **(B)** Ankle thickness was determined at day 7 post-STA and normalized to day 0. **(C)** H&E staining, inflammation score, and quantification of inflammation area of hind paw ankle talus sections on day 10 post-STA. Black arrowheads indicate the area of inflammatory cell infiltration and synovial membrane hyperplasia. Ti: tibia, Ta: talus, Sm: synovial membrane. Scale bar: 500 μm. **(D)** mRNA expression of *Il1b, Il6, Ifng, Nos2, Cxcr2,* and *Cxcr4* in arthritic joints from $Tfr2^{+/+}$ and $Tfr2^{-/-}$ mice. **(E)** Heat map representation of cytokines, chemokines, and inflammatory proteins profile in serum from arthritic $Tfr2^{+/+}$ and $Tfr2^{-/-}$ mice. Data are presented as mean ± SD. Student's *t*-test or two-way ANOVA (followed by the post hoc Bonferroni's test). Each symbol represents an individual animal. *$P < 0.05$, **$P < 0.01$, ***$P < 0.001$. . (For interpretation of the references to colour in this figure legend, the reader is referred to the Web version of this article.)
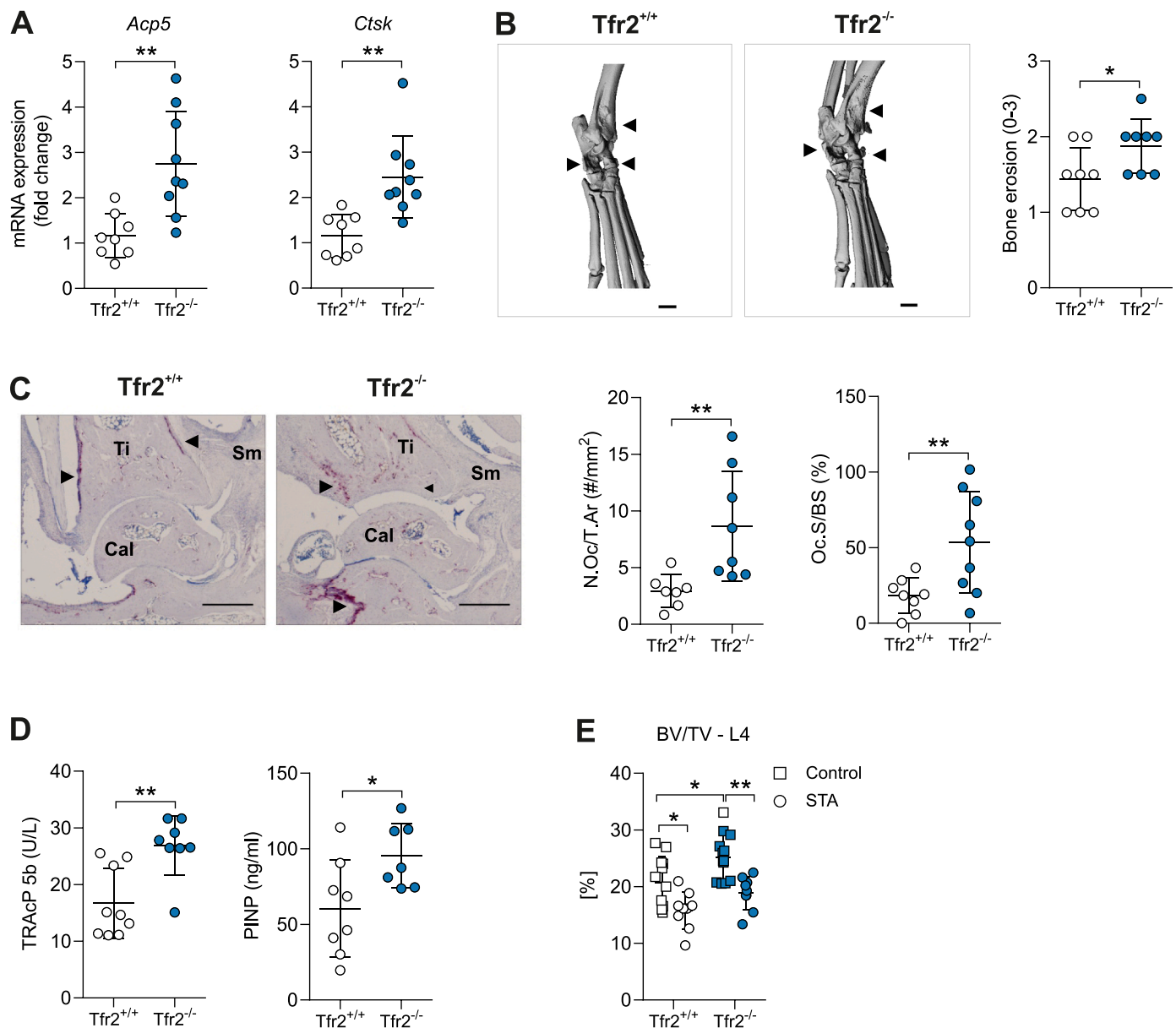
Fig. 2. *Tfr2*-deficient mice display enhanced bone erosion in inflammatory arthritis.
(A) Expression of *Acp5* and *Ctsk* mRNA analyzed in the total paw extracts from *Tfr2*$^{+/+}$ (n = 8, white symbols) and *Tfr2*$^{-/-}$ (n = 9, blue symbols) male mice at day 10 post-K/BxN serum-transfer arthritis (STA) by quantitative RT-PCR. **(B)** Representative μ-CT images of mouse ankle at day 10 post-STA, and bone erosion score determined at the tibiotalar area. Black arrowheads denote bone erosion. Scale bar: 1 mm. **(C)** Tartrate-resistant acid phosphatase staining, and quantification of the number of osteoclasts as well as osteoclast surface in the hind paws of *Tfr2*$^{+/+}$ and *Tfr2*$^{-/-}$ mice at day 10 post-STA. Black arrowheads indicate osteoclast in the synovial space. Ti: tibia, Ca: calcaneus, Sm: synovial membrane. Scale bar: 500 μm. **(D)** TRAcP 5 b and P1NP serum levels in *Tfr2*$^{+/+}$ and *Tfr2*$^{-/-}$ mice. **(E)** μCT analysis of the trabecular bone volume per total volume (BV/TV) at the fourth vertebral body of arthritic and healthy *Tfr2*$^{+/+}$ and *Tfr2*$^{-/-}$ male mice at day 10 post-STA. Data are presented as mean ± SD. Student's *t*-test or two-way ANOVA (followed by the post hoc Bonferroni's test). Each symbol represents an individual animal. *$P < 0.05$, **$P < 0.01$. . (For interpretation of the references to colour in this figure legend, the reader is referred to the Web version of this article.)

when compared with the inflamed joints of *Tfr2*$^{+/+}$ mice on day 7 (Fig. 3B). Further analysis revealed that the frequency of neutrophil (CD45$^+$CD11b$^+$Ly6G$^+$) (Fig. 3C) and monocyte/macrophage (CD45$^+$CD11b$^+$F4/80$^+$) populations (Fig. 3D) was enhanced in the arthritic joints from *Tfr2*$^{-/-}$ compared to *Tfr2*$^{+/+}$ mice, which suggest that lack of *Tfr2* is associated with a more pronounced development of arthritis, likely due to enhanced neutrophil and monocyte/macrophage cell infiltration into the joint.

3.3. Specific deletion of Tfr2 in neutrophils and macrophages affects arthritis disease severity

Since STA initiation and progression are dependent on innate immune cells, such as neutrophils and macrophages [26], and the recruitment of these cells was significantly increased in the inflamed joints of *Tfr2*$^{-/-}$ mice, we sought to discover in which cell type Tfr2 function was dampening arthritis progression. As *Tfr2* is expressed in neutrophils and macrophages (Fig. S4A), we generated mice with a specific inactivation of *Tfr2* in the myeloid lineage (*Tfr2*$^{fl/fl}$; *LysM-Cre* +)
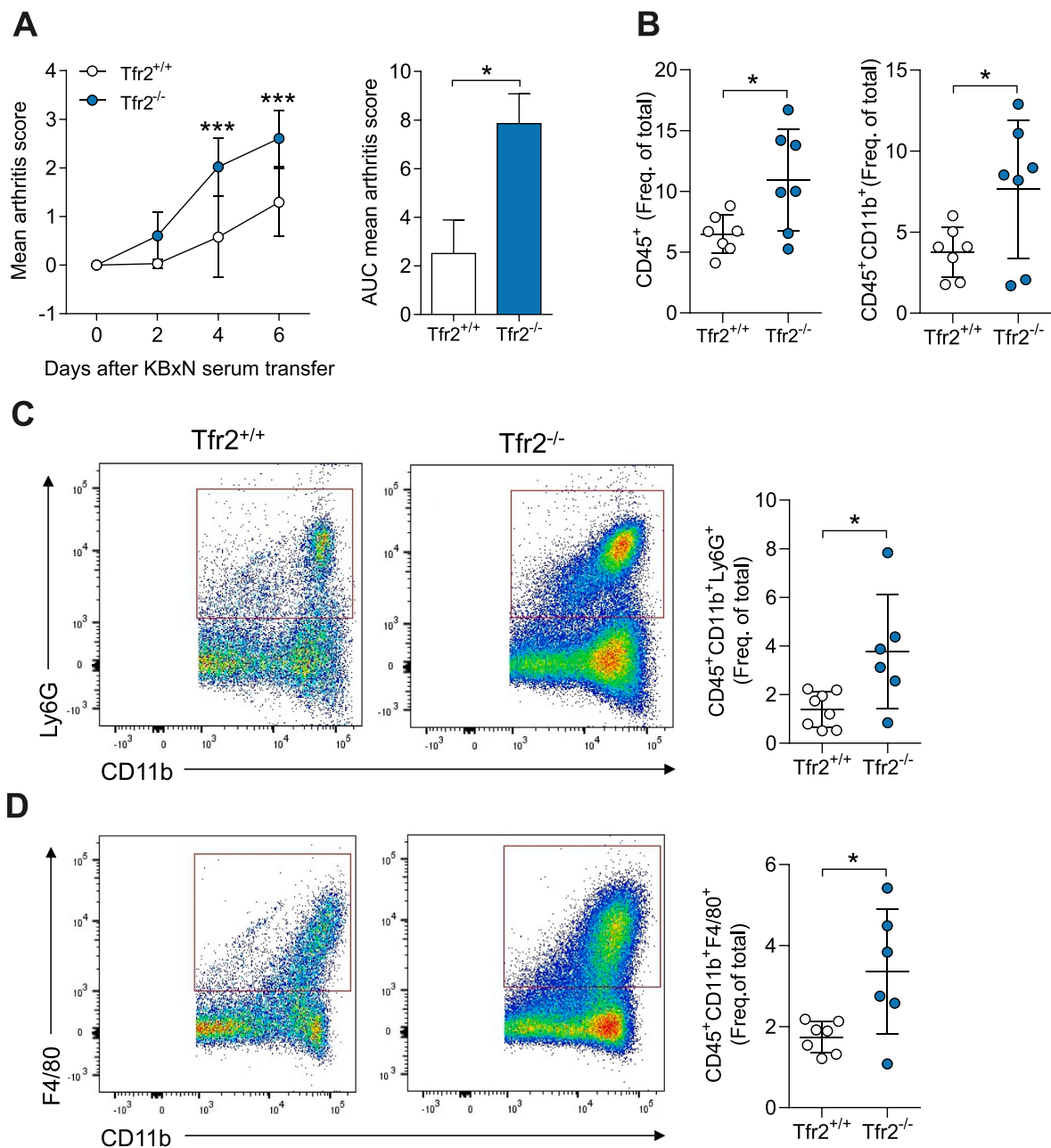
Fig. 3. *Tfr2*-deletion promotes neutrophil and macrophage infiltration to inflamed joints.
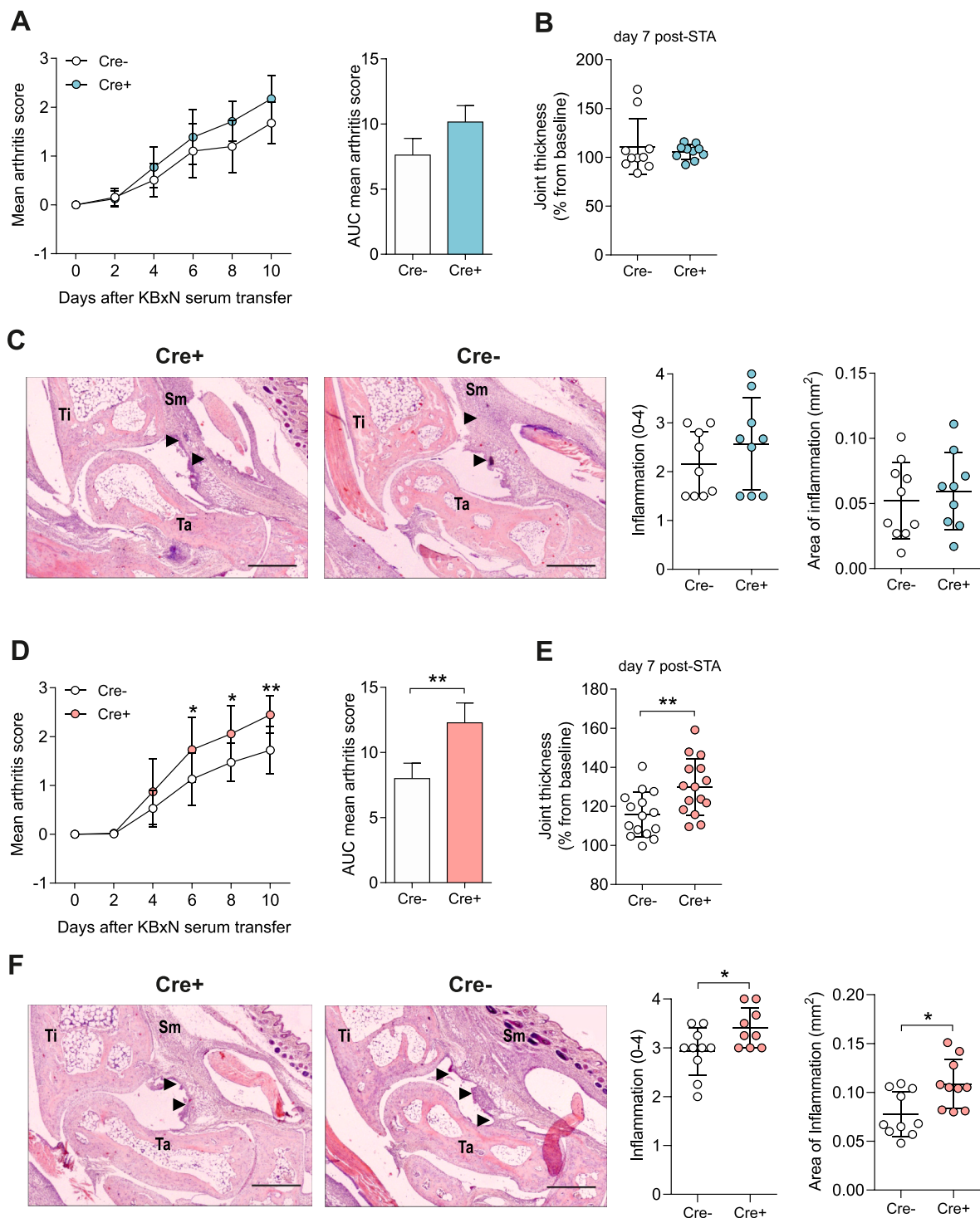**(A)** Arthritis progression assessed by mean clinical scores of *Tfr2*$^{+/+}$ (n = 7, white symbols) and *Tfr2*$^{-/-}$ (n = 7, blue symbols) male mice at day 7 post-K/BxN serum-transfer arthritis (STA), and area under the curve (AUC). **(B)** Frequency of hematopoietic (CD45$^+$) and myeloid cells (CD45$^+$CD11b$^+$) in the joints of *Tfr2*$^{+/+}$ and *Tfr2*$^{-/-}$ mice after 7 days of STA-challenge. **(C)** Representative plots and frequency of neutrophils (CD45$^+$CD11b$^+$Ly6G$^+$) and **(D)** macrophages (CD45$^+$CD11b$^+$F4/80$^+$) in the joints of *Tfr2*$^{+/+}$ and *Tfr2*$^{-/-}$ mice at day 7 post-STA. Data are presented as mean ± SD. Student's *t*-test or two-way ANOVA (followed by the post hoc Bonferroni's test). Each symbol represents an individual animal. *$P < 0.05$, ***$P < 0.001$. . (For interpretation of the references to colour in this figure legend, the reader is referred to the Web version of this article.)

(Fig. S4B), which importantly has been previously characterized with normal iron loading (Table S4). *Tfr2*$^{fl/fl}$; *LysM-Cre* + male mice developed arthritis that was comparable to their Cre-negative counterpart littermates (Fig. 4A and B). Consistent with these observations, histological examination of tibiotalar joints on day 10 post-STA demonstrated a similar extent of inflammation (Fig. 4C). Intriguingly, *Tfr2*$^{fl/fl}$; *LysM-Cre* + female mice exhibited significantly higher clinical scores and joint swelling compared to *Tfr2*$^{fl/fl}$; *LysM-Cre*-female mice (Fig. 4D and E). In addition, histological analysis exhibited increased cellular infiltrates and synovial inflammation in *Tfr2*$^{fl/fl}$; *LysM-Cre* + female mice (Fig. 4F).

Thus, *Tfr2* expression in myeloid cells regulates inflammatory arthritis severity.

3.4. Deletion of Tfr2 in macrophages promotes M1-like polarization driven by IFN-γ

To further investigate how Tfr2 might affect neutrophil and macrophage function during inflammatory arthritis, we collected neutrophils from *Tfr2*$^{+/+}$ and *Tfr2*$^{-/-}$ healthy mice and incubated them for 4 h in the presence of TNFα (used to elicit a pro-inflammatory response). No

Fig. 4. *Tfr2* expression in myeloid cells regulates disease severity in inflammatory arthritis.

(A) Arthritis progression assessed by mean clinical scores of male *Tfr2*^fl/fl *(Cre-)* and *Tfr2*^fl/fl *LysM (Cre +)* mice injected with K/BxN serum (STA), and area under the curve (AUC). **(B)** Ankle thickness was determined at day 7 post-STA and normalized to day 0. **(C)** H&E staining, inflammation score, and quantification of inflammation area of hind paw ankle talus sections on day 10 post-STA. Black arrowheads indicate the area of inflammatory cell infiltration and synovial hyperplasia. Ti: tibia, Ta: talus, Sm: synovial membrane. Scale bar: 500 μm. Cre- (n = 10), Cre+ (n = 9). **(D)** Arthritis progression assessed by mean clinical scores of female *Tfr2*^fl/ fl *(Cre-)* and *Tfr2*^fl/fl *LysM (Cre +)* mice injected with K/BxN serum (STA), and AUC. **(E)** Ankle thickness determined at day 7 post-STA and normalized to day 0. **(F)** H&E staining, inflammation score, and quantification of inflammation area of hind paw ankle talus sections on day 10 post-STA. Black arrowheads indicate the area of inflammatory cell infiltration and synovial hyperplasia. Ti: tibia, Ta: talus, Sm: synovial membrane. Scale bar: 500 μm. Cre- (n = 10), Cre+ (n = 9). Data are presented as mean ± SD. Each symbol represents an individual animal. Student's *t*-test or two-way ANOVA (followed by the post hoc Bonferroni's test). *$P < 0.05$, **$P < 0.01$.

differences were observed between the mRNA expression levels of the pro-inflammatory markers *Tnfa*, *Il1b*, *Nos2*, and *Cxcl2* after TNFα (Fig. S5A) or LPS stimulation (Fig. S5B). To evaluate phagocyte function and reactive oxygen species (ROS) production, neutrophils were stimulated with either LPS (for phagocytosis) or PMA (for total ROS). *Tfr2$^{-/-}$* neutrophils showed an increased capacity of phagocytic activity after 2 h of LPS stimulation compared with *Tfr2$^{+/+}$* neutrophils (Fig. S5C). Moreover, *Tfr2$^{-/-}$* neutrophils showed an enhanced capacity to produce ROS after PMA activation (Fig. S5D). Therefore, these results suggest that the lack of *Tfr2* in neutrophils does not alter the production of pro-inflammatory molecules induced by either TNFα or LPS during the inflammatory response, but regulates their antimicrobial activity.

Macrophages are key players involved in the regulation of iron availability to properly facilitate inflammatory responses. Therefore, we next analyzed whether the lack of *Tfr2* in these cells influences their polarization and function contributing to inflammation and arthritis progression via M1-like phenotype activation. We examined the transcriptional response of *Tfr2*-deficient macrophages induced by IFN-γ (used as M1-like activator). BMDM from *Tfr2$^{-/-}$* or *Tfr2$^{+/+}$* mice were cultured *in vitro* for 6 days. Then, cells were activated with IFN-γ (100 ng/mll) and examined for gene expression. Activation with IFN-γ induced *Tfr2* expression in wild-type macrophages (Fig. 5A), and enhanced the mRNA expression of the M1-like marker genes including *Nos2*, *Tnfa*, *Icam1*, *Socs1*, and *Socs3* in *Tfr2$^{-/-}$* BMDM compared to *Tfr2$^{+/+}$* BMDM (Fig. 5B). IFN-γ also increased the expression of IFN-γ-inducible genes *Cxcl9*, *Cxcl11*, *Ccl12*, *Irf1,* and *Irf8*, while *Cxcl10* remained unchanged (Fig. 5C). In addition to cytokines, pro-inflammatory macrophages produce large amounts of NO, a cytotoxic mediator used in host defense and intracellular metabolism [27]. As expected from the increased expression of *Nos2, Tfr2$^{-/-}$* macrophages secreted larger amounts of NO compared to *Tfr2$^{+/+}$* macrophages upon IFN-γ stimulation (Fig. 5D). In the absence of *Tfr2*, macrophages stimulated with LPS during 24 h showed increased phagocytosis, as determined by the engulfment of zymosan conjugated particles (Fig. 5E), while its redox activity remained unchanged (Fig. 5F). Furthermore, IFN-γ functions are mediated by direct activation of immune effector genes via the JAK-STAT1 signaling pathway [28]. Consistently, we observed that deletion of *Tfr2* in macrophages led to enhanced and prolonged IFN-γ-induced STAT1-activation (Fig. 5G). Since iron can also fine-tune the innate immune response in macrophages, we investigated whether Tfr2-deficiency influences macrophage intracellular iron content that could contribute to macrophage M1-like pro-inflammatory polarization. Iron content in macrophages showed that *Tfr2$^{-/-}$* cells are iron deficient compared to *Tfr2$^{+/+}$* cells (Fig. S6A). Importantly, the mRNA levels of *Fpn1* were increased in control *Tfr2$^{-/-}$* cells, *Tfrc* expression was decreased (Fig. S6C). *Fth1* mRNA and protein expression remained unchanged when compared to *Tfr2$^{+/+}$* cells (Figs. S6B and C), while 24 h treatment with IFN-γ diminished those effects in both genotypes. To further analyze the participation of iron in the effect of Tfr2-deficiency on macrophage M1-like polarization, BMDM were treated with ferric ammonium citrate (FAC) to provide a source of iron that resulted in iron loading in both genotypes (Fig. S6D), after which IFN-γ was added. While the enhanced phosphorylated STAT1 signaling was reduced by iron (Fig. S6E), the induced expression of pro-inflammatory cytokines (*Nos2, Tnfa, Cxcl9, Cxcl11*) in Tfr2-deficient cells could not be rescued (Fig. S6F), suggesting iron independent effect in the Tfr2-dependent regulation of pro-inflammatory genes.

Furthermore, our observations that Tfr2 is required to restrain macrophage pro-inflammatory activation prompted us to investigate whether this protein is also involved in macrophage anti-inflammatory activation. Stimulation of *Tfr2$^{+/+}$* and *Tfr2$^{-/-}$* macrophages with IL-4 revealed no differences in the expression of anti-inflammatory-related genes, such as Arg*1*, *Ym1*, *Fizz1*, *Mrc1* (Fig. S7A) and did not modify the expression of the inflammatory markers *Nos2* and *Tnfa* (Fig. S7B). Taking together, these results indicate that macrophages deficient in *Tfr2* display increased sensitivity to M1-like classically polarizing stimuli such as IFN-γ, suggesting that Tfr2 plays a negative role in M1-like macrophage differentiation.

### 3.5. Tfr2-dependent IFNγ-induced M1-like macrophage polarization is controlled by JAK1/2 signaling

Because lack of *Tfr2* increases macrophage sensitivity to IFN-γ, which activates STAT1, we tested whether the observed STAT1-activation was directly responsible for this pro-inflammatory phenotype. We inhibited STAT1 Y701 phosphorylation using the JAK1/2 inhibitor Ruxo and hypothesized that by inhibiting this response, the M1-like phenotype in *Tfr2*-deficient macrophages might be abrogated. To test this hypothesis, we pre-treated *Tfr2* sufficient and deficient macrophages with 0.1 and 0.5 μM Ruxo, and challenged them with IFN-γ for 6 h. Co-treatment with Ruxo resulted in a dose-dependent inhibition of STAT1 Y701 phosphorylation. Levels of phosphorylated STAT1 were significantly down-regulated regardless of *Tfr2*-deletion (Fig. 6A). We further investigated the implication of STAT1 inhibition in inflammatory macrophages. Treatment with Ruxo inhibited M1-like polarization in both *Tfr2$^{+/+}$* and *Tfr2$^{-/-}$* macrophages as illustrated in mRNA expression of M1-like specific signature markers: *Nos2*, *Tnfa*, *Icam1*, *Socs1*, *Socs3* (Fig. 6B)*,* as well as the expression of specific IFN-γ target genes, including *Cxcl9*, *Cxcl11*, *Ccl12*, and *Irf8*, while *Irf1* remained unchanged (Fig. 6C). Furthermore, exposure to Ruxo resulted in lowered NO production (Fig. 6D), confirming that JAK1/2 inhibition attenuated the enhanced response of *Tfr2*-deficient macrophages mediated by IFN-γ stimulation.

Subsequently, we investigated the capacity of IFNγ-treated *Tfr2$^{+/+}$* and *Tfr2$^{-/-}$* macrophages to secrete pro-inflammatory cytokines, chemokines, and other inflammatory molecules in conditioned culture media in the presence or absence of Ruxo. Results after 18 h of culture are shown in Fig. 6E. Of the 40 pro-inflammatory markers assessed, 16 were elevated at least 2-fold in *Tfr2$^{-/-}$* macrophages as compared with the levels in *Tfr2$^{+/+}$* macrophages, suggesting a key role of Tfr2 in repressing the secretion of cytokines (IL4, IL-6, IL-7, IL16, IL-17, IL-27), chemokines (CXCL1, CCL3, CXCL9, CXCL10, CXCL11, CXCL13) and inflammatory proteins (GM-CSF, M-CSF, sCAM-1, C5/5a, TIMP-1, TREM-1), while this upregulation is abrogated by the pre-treatment with Ruxo. Quantitative pixel analysis of the investigated cytokines is shown in Table S5. Taken together, these data indicate that the striking pro-inflammatory changes displayed in *Tfr2*-deficient macrophages following exposure to IFN-γ are key drivers of inflammation, and likely contribute to arthritis progression.

4. Discussion

RA is a complex autoimmune disease characterized by chronic inflammation in which prolonged immune cell activation is largely responsible for synovial iron sequestration and anemia [5]. Moreover, previous work has implicated an accumulation of iron in the arthritic joint as a cause of increased inflammation. Patients with RA have demonstrated worsening of the disease after iron supplementation to correct anemia, while a small number of studies in humans and animal models have demonstrated some improvement of disease activity with iron-chelating agents [6–9]. Thus, iron could contribute to a vicious cycle of inflammatory processes in arthritis.

Tfr2 is a critical regulator of iron homeostasis and has also been implicated to regulate bone turnover [16]. Thus, we investigated the role of Tfr2 and iron overload, which occurs due to Tfr2 deficiency, in arthritis and arthritis-induced bone loss. Our results indicate that *Tfr2*-deficiency aggravates the inflammatory response in arthritis. In contrast to wild-type littermates, *Tfr2$^{-/-}$* mice developed more severe arthritis characterized by increased synovitis, massive recruitment of neutrophils and macrophages, and structural joint damage, suggesting a role of Tfr2 and/or iron overload in the pathogenesis of arthritis. Interestingly, only male, but not female *Tfr2$^{-/-}$* mice showed an
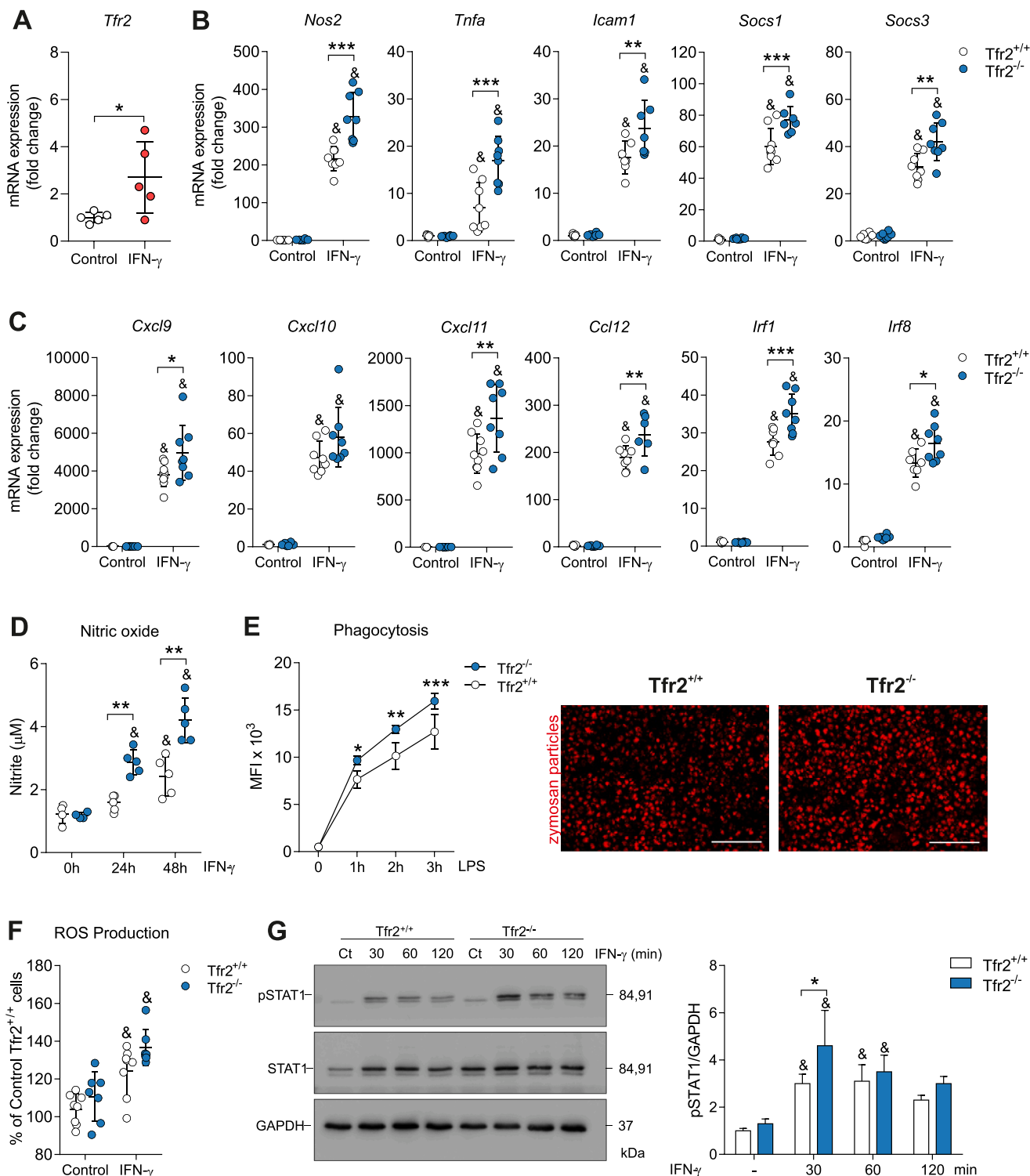
Fig. 5. IFN-γ-treated macrophages show enhanced M1-like phenotype activation in the absence of Tfr2.
(A) mRNA expression of *Tfr2* in wild-type in bone marrow-derived macrophages (BMDM) stimulated with IFN-γ (100 ng/ml) for 24 h, **(B)** mRNA levels of M1-like gene signatures (*Nos2, Tnfa, Icam1, Socs1, Socs3*) and **(C)** IFN-γ-target genes (*Cxcl9, Cxcl10, Cxcl11, Ccl2, Irf1, Irf8*) were measured in BMDM from *Tfr2*$^{+/+}$ and *Tfr2*$^{-/-}$ male mice after IFN-γ stimulation for 6 h. **(D)** Nitric oxide secretion by *Tfr2*$^{+/+}$ and *Tfr2*$^{-/-}$ BMDM treated with IFN-γ for 24 h and 48 h. **(E)** Phagocytosis index of zymosan particles and representative images obtained after 3 h incubation of BMDM from *Tfr2*$^{+/+}$ and *Tfr2*$^{-/-}$ mice stimulated for 24 h with LPS (100 ng/ml). Scale bar: 200 μm. **(F)** ROS production by *Tfr2*$^{+/+}$ and *Tfr2*$^{-/-}$ BMDM treated or not with IFN-γ for 3 h. **(G)** Western blot for phosphorylated STAT1 and total STAT1 protein in *Tfr2*$^{+/+}$ and *Tfr2*$^{-/-}$ BMDM left untreated or stimulated with IFN-γ for 30, 60, and 120 min. The graph on the right: fold change in GAPDH-normalized phosphorylated-STAT1 band intensity relative to untreated BMDM. The blot shown is representative of two independent experiments. Data are presented as mean ± SD. Each symbol represents macrophages differentiated from an individual animal. Student's *t*-test or two-way ANOVA (followed by the post hoc Bonferroni's test). $^{\&}P < 0.001$ vs. untreated control BMDM; $*P < 0.05$, $**P < 0.01$, $***P < 0.001$.
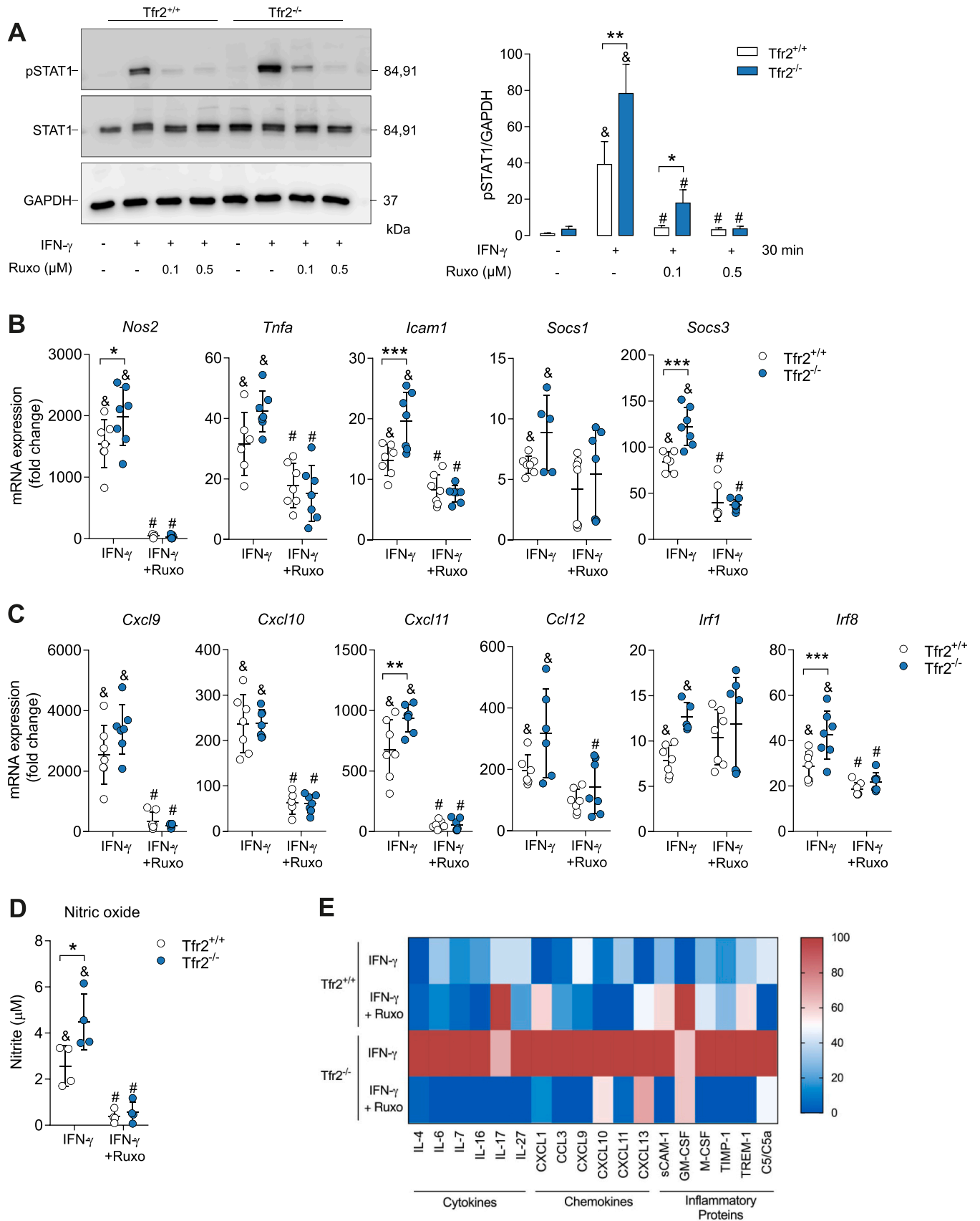
(caption on next page)

Fig. 6. Tfr2-dependent IFN -γ-induced macrophage polarization is JAK1/2-dependent.
(A) Western blot for phosphorylated STAT1 and total STAT1 protein in $Tfr2^{+/+}$ and $Tfr2^{-/-}$ bone marrow-derived macrophages (BMDM) left untreated or stimulated with IFN-γ (100 ng/ml) for 30 min in the presence or absence of the JAK1/2 inhibitor ruxolitinib (Ruxo; 0.1 μM or 0.5 μM). The graph on the right: fold change in GAPDH-normalized phosphorylated STAT1 band intensity relative to untreated BMDM. **(B)** mRNA cytokine levels of inflammatory gene signatures (*Nos2*, *Tnfa*, *Icam1*, *Socs1*, *Socs3*) and **(C)** IFN-γ-target genes (*Cxcl9*, *Cxcl10*, *Cxcl11*, *Ccl2*, *Irf1*, *Irf8*) were measured in BMDM from $Tfr2^{+/+}$ and $Tfr2^{-/-}$ after IFN-γ stimulation for 6 h ± 1 h pre-treatment with Ruxo (0.1 μM). **(D)** Nitric oxide secretion by $Tfr2^{+/+}$ and $Tfr2^{-/-}$ BMDM treated with IFN-γ for 48 h ± 1 h pre-treatment with Ruxo (0.1 μM). **(E)** BMDM from $Tfr2^{+/+}$ and $Tfr2^{-/-}$ mice were stimulated with IFN-γ for 18 h ± 1 h pre-treatment with Ruxo (0.1 μM). Heat map representation of cytokines, chemokines, and inflammatory proteins profile measured in conditioned media using a cytokine array dot blot. Data are presented as mean ± SD. Each symbol represents macrophages differentiated from an individual animal. Student's *t*-test or two-way ANOVA (followed by the post hoc Bonferroni's test). $^{\&}P < 0.001$ vs. untreated control BMDM, $^{\#}P < 0.001$ vs. IFN-γ treated BMDM, $^{*}P < 0.05$, $^{**}P < 0.01$, $^{***}P < 0.001$.

increased disease severity. Previous studies have shown sexual disparities in iron metabolism in humans and experimental animals, with females, having lower iron stores, and being more resistant to iron overload-mediated injury and adverse clinical outcomes than males [29,30]. While this is a novel description of the iron sensor Tfr2 in chronic inflammation, previous reports have suggested that elevated iron stores worsen the response to infection and inflammation [31]. As such, iron overload associated with hereditary hemochromatosis in humans and mice has been reported to confer susceptibility to siderophilic bacteria and influence the course of viral infections [32]. Furthermore, increased iron stores are correlated with markers of chronic inflammation and risk factors for diabetes, chronic liver disease, and atherosclerosis, while iron chelation treatment may confer clinical benefits [33]. Taken together, these reports suggest an influence of iron on the course of inflammation and likely in the pathogenesis of arthritis in *Tfr2*-deficient mice.

Oxidative stress occurs in iron overload, with a decrease of antioxidants and an increase of ROS. Likewise, a larger number of studies have highlighted the role of oxidative stress in the pathophysiology of RA [22, 23]. To elucidate the participation of iron overload in Tfr2-deficient mice with arthritis conditions, we measured anti-oxidative stress enzymes in joints and liver. While at the level of the joints no significant changes were observed, livers from healthy and STA *Tfr2*-deficient mice did not show an increase of expression of anti-oxidant genes in contrast to $Tfr2^{+/+}$ STA mice, suggesting that the oxidative stress response is not involved in the increased susceptibility to arthritis development in Tfr2-deficient mice.

To further address the impact of iron overload in our model, we used myeloid-specific *Tfr2*-deficient mice as $Tfr2^{-/-}$ mice showed an increased presence of myeloid cells in inflamed joints and these mice have previously shown to have normal iron loading [15]. Myeloid-specific deletion of *Tfr2* in female mice also resulted in more severe arthritis, suggesting a cell-intrinsic and iron-independent role of Tfr2 in arthritis. Studies addressing gender imbalance in RA development have demonstrated that females showed an increased response to pro-inflammatory hormones [34] and enhanced immunoreactivity compared to males with higher immunoglobulin levels and enhanced antibody production to antigen stimulation [35], factors that could explain the preponderance of arthritis observed in *Tfr2;LysMCre* female mice. However, as $Tfr2^{-/-}$ mice showed more severe arthritis as compared to myeloid-specific *Tfr2*-deficient mice, the role of iron overload in arthritis development cannot be fully excluded.

Since our results indicated that Tfr2 in myeloid cells influences arthritis progression, we investigated the role of Tfr2 in neutrophils and macrophages more carefully, as both cell types are targeted by the LysM-Cre. Neutrophil activation is critical for the induction and progression of STA [36]. After entry into the inflammatory site, in response to pro-inflammatory stimuli, neutrophils become fully activated, a state characterized by the release of degradative enzymes, pro-inflammatory cytokines, and acquisition of phagocytic function and ROS generation [37]. We showed that *Tfr2*-deletion leads to enhanced neutrophil migration into the joint cavity in STA, but has no effects on the production of pro-inflammatory factors mediated by these cells. *In vitro* challenge with TNFα or LPS resulted in a similar induction of pro-inflammatory cytokines, while LPS-induced phagocyte activity and

PMA-induced ROS production were further enhanced in *Tfr2*-deficient neutrophils. These results are in line with earlier reports showing that neutrophils from hereditary hemochromatosis patients have normal iron loading but are primed by circulating TNFα and that this is associated with an increased oxidative burst capacity and phagocytosis [38].

Besides neutrophils, macrophages play a crucial role in STA development. Depending on phenotype and secreted cytokines, macrophages are broadly classified as M1-like (pro-inflammatory) and M2-like (anti-inflammatory). In particular, infiltration of circulating monocytes and subsequent differentiation are critical processes for exacerbation of RA [39]. Here, we demonstrated that *Tfr2*-deficiency leads to enhanced macrophage recruitment in STA and this upregulation was associated with increased expression of pro-inflammatory factors in the systemic circulation. Consistent with these findings, gene expression analysis showed that mRNA levels of numerous M1-like marker genes were highly elevated in the joint tissues of $Tfr2^{-/-}$ mice. These *in vivo* results were consistent with the *in vitro* data showing enhanced M1-like polarization through IFN-γ-mediated STAT1 activation in $Tfr2^{-/-}$ macrophages, resulting in downstream gene expression and production of pro-inflammatory cytokines and NO. Furthermore, we established that specific STAT1 inhibition by ruxolitinib (Ruxo) reduces M-like macrophage activation in $Tfr2^{-/-}$ macrophages. IFN-γ is a key modulator of macrophage immune function and iron status [40]. Macrophages respond to IFN-γ by inducing the expression of iNOS, the key enzyme in NO production that is dependent on host cell iron status. Increased iron results in inhibition of iNOS activity while iron deficiency enhances its activity [41]. In agreement with these reports, *Tfr2*-deficient macrophages showed increased expression of iNOS and enhanced production of NO. Moreover, whether the observed effects are mediated via Tfr2 controlling cellular iron pools remains to be investigated. Interestingly, it has been reported that *Tfr2*-deficiency in mice and humans results in splenic iron deficiency due to low hepcidin levels that stabilize the iron exporter FPN, suggesting that *Tfr2*-deficient macrophages are relatively iron-depleted, despite systemic iron overload [15,42]. In line with these findings, we have observed lower iron content in $Tfr2^{-/-}$ macrophages compared to wild-type cells. Surprisingly, $Tfr2^{-/-}$ cells paradoxically upregulated the iron exporter Fpn and downregulate the iron importer Tfr1 (encoded by the *Tfrc* gene) despite the lack of iron, suggesting a different response of these cells to iron deprivation, a condition that has been also reported in skeletal muscle cells [43]. Moreover, supplementation of iron indeed mitigated the enhanced IFN-γ-mediated STAT1 activation in *Tfr2*-deficient macrophages, but even further enhanced the expression of downstream gene expression. This suggests that in the absence of STAT1, IFN-γ can still regulate the expression of some genes through other STAT1-independent pathways [44].

No differences were observed in the ability of IL-4 to promote the expression of M2-macrophages gene markers. IL-4 promoted M2 polarization in *Tfr2*-deficient macrophages to the same extent as in *Tfr2* wild-type cells. These results indicate that in absence of Tfr2, macrophages have an increased sensitivity to inducers of the M1-like phenotype such as IFN-γ, while the ability to respond to the M2 phenotype inducer IL-4 is not altered.

Besides arthritis, other iron overload disorders such as thalassemia have deleterious effects on bone metabolism. Clinical studies and mouse models have revealed an increased fracture risk characterized by low

bone mass, suppressed bone formation, and increased bone resorption [45,46]. Interestingly, among several mouse models of hemochromatosis that show low bone mass [47–49], *Tfr2*-deficient mice have a high bone mass with increased bone formation and resorption activities [16]. Due to the higher bone mass of $Tfr2^{-/-}$ mice, we speculated that they might be protected from arthritis-induced bone loss. However, during arthritis, osteoclast activity was even further enhanced in $Tfr2^{-/-}$ mice, leading to more severe bone loss than in wild-type animals. Similar results were seen in the context of estrogen deficiency, in which the high bone turnover of $Tfr2^{-/-}$ mice resulted in even more bone loss than wild-type controls [16]. As Tfr2 is highly upregulated during osteoclastogenesis, a cell-intrinsic role of Tfr2 in osteoclasts can also be envisaged. Moreover, iron is crucial for proper osteoclast differentiation and increased iron concentrations accelerate their differentiation and activity [50]. Thus, whether this is an effect mediated by Tfr2 actions mediating intracellular iron storage remains to be elucidated.

In conclusion, we have shown that *Tfr2* deficiency supports M1-like macrophage polarization under inflammatory conditions and thus, leads to more severe arthritis in mice, an effect that is largely independent of iron, suggesting an important extrahepatic role for Tfr2.

Authors contributions

All authors were involved in drafting the article or revising it critically for important intellectual content, and all authors approved the final version. Dr. Rauner had full access to all of the data in the study and takes responsibility for the integrity of the data. **Study conception and design:** Ledesma-Colunga, Baschant, Rauner. **Acquisition of data:** Ledesma-Colunga, Baschant, Weidner, Alves, Mirtschink. **Analysis and interpretation of data:** Ledesma-Colunga; Baschant, Weidner, Alves, Mirtschink, Hofbauer, Rauner.

Financial support

Declaration of competing interest

LCH received support for clinical trials to his institution from Alexion, Ascendis, Takeda, and UCB. MR received honoraria for lectures from UCB. All other authors have no financial conflicts of interest.

Table S1
Primers for quantitative PCR.

Gene	Forward (5' - 3')	Reverse (5' - 3')
Tnfa	GCTGAGCTCAAACCCTGGTA	CGGACTCCGCAAAGTCTAAG
Il1b	ACAAGGAGAACCAAGCAACG	GCCGTCTTTCATTACACAGG
Il6	ACTTCCATCCAGTTGCCTTC	ATTTCCACGATTTCCCAGAG
Nos2	CAGCTGGGCTGTACAAACCTT	CATTGGAAGTGAAGCGTTTCG
Ifng	GCGTCATTGAATCACACCTG	GACCTGTGGGTTGTTGACCT
Tfr2	GCCATGTTTCTCCCGGTTCCT	TGGCGCGAGAGCTTATCG
Acp5	ACTTGCGACCATTGTTAGCC	AGA GGG ATC CAT GAA GTT GC
Ctsk	AAGTGGTTCAGAAGATGACGGGAC	TCTTCAGAGTCAATGCCTCCGTTC
Icam1	CCTGTTTCCTGCCTCTGAAG	CTGCTGTTTGTGCTCTCCTG
Cxcr4	TACATCTGTGACCGCCTTTA	GGCAAAGAAAGCTAGGATGA
Cxcr2	GTGCATAGCCATGTGGTTAC	GGCAGGATACGCAGTACG
Socs1	ACCTTCTTGGTGCGCGAC	GGGCCCGAAGCCATCTT
Irf1	TTTGAACAGTCTGAGTGGCA	ATCTCCGTGAAGACATGTTGT
Irf8	AAGGAACCTTCTGTGGATGAGTA	AAGCTGAATGGTGTGTGTCA
Ccl12	TGTTAAGCAGAAGATTCACGTCC	AAGGATGAAGGTTTGAGACGT
Cxcl9	TCGGCAAATGTGAAGAAGCT	ACTTTGGGGTGTTTTGGGTT
Cxcl10	GCTGCAACTGCATCCATATC	TTTCATCGTGGCAATGATCT
Cxcl11	TCATAAACGACAAAGGTGCCT	TCCCAGGATGTCACATGTTTT
Socs3	TCAAGACCTTCAGCTCCAAAA	TTGACGCTCAACGTGAAGAA

(continued on next column)

Table S1 (*continued*)

Gene	Forward (5' - 3')	Reverse (5' - 3')
Fizz1	AACTATCCCTCCACTGTAACGAA	ATCATATCAAAGCTGGGTTCTCC
Mrc1	TCACTGATGCAAACCACACA	TCGGCATTCCAGTGTGTAAA
Ym1	TCCTCAGAACCGTCAGATATTCA	AGCAGCCTTGGAATGTCTTT
Arg1	CTATGTGTCATTTGGGTGGA	CACGATGTCTTTGGCAGATA
Hmox1	CCACCAAGTTCAAACAGCTCTAT	TTTGTGTTCCTCTGTCAGCATCA
Nrf2	TGGCAGAGACATTCCCATTT	ACACTGTAATTCGGGAATGGA
Nqo1	GATGGGAGGTACTCGAATCTG	TCAGCTCACCTGTGATGTC
Gsr	ACGACCATGATTCCAGATGTT	AGCATAGACGCCTTTGACAT
Gsta1	ATGTTTGACCAAGTGCCCAT	TGCCCAATCATTTCAGTCAGA
Txn2	AGTTGTTGTGGACTTTCATGCA	TTCAATGGCAAGGTCTGTGT
Sod2	AATCTCAACGCCACCGAGGA	TCTCCTTTGGGGTTCTCCACCA
Cat	TTTTCACTGACGAGATGGCA	AAACACCTTTGCCTTGGAGT
Tfrc	TAAATTCCCCGTTGTTGAGG	ATGACTGAGATGGCGGAAAC
Fpn1	TGTCAGCCTGCTGTTTGCAGGA	TCTTGCAGCAACTGTGTCACCG
Fth1	CTTCGAGCCTGAGCCCTTTG	CAGGTTGATCTGGCGGTTGA
Gpx4	ATGCACGAATTCTCAGCCAA	TCAGTTTTGCCTCATTGCGA
Actb	GATCTGGCACCACACCTTCT	GGGGTGTTGAAGGTCTCAAA
Gapdh	AAGGTCATCCCAGAGCTGAA	CTGCTTCACCACCTTCTTGA

Table S2

Hematological and iron parameters for $Tfr2^{+/+}$ and $Tfr2^{-/-}$ male and female mice subjected to K/BxN serum transfer induced arthritis (STA).

Male	$Tfr2^{+/+}$		$Tfr2^{-/-}$	
	Control (n = 8)	STA (n = 5)	Control (n = 8)	STA (n = 5)
Liver Fe (µg/g)	232.1 ± 45.4	253.7 ± 99.3	1713.7 ± 303.6***	1299.1 ± 373.7***,#,&
Spleen Fe (µg/g)	1989.6 ± 410.6	1485.9 ± 458.4	1436.1 ± 234.2	1046.5 ± 342.2***
Serum Fe (µg/dL)	144.9 ± 37.1	145.2 ± 47.1	211.7 ± 22.2*	208.0 ± 44.5*,&
Transferrin Saturation (%)	41.3 ± 8.0	50.3 ± 10.5	76.0 ± 20.3***	79.3 ± 10.5***,&
Liver *Hamp* mRNA	1.0 ± 0.3	1.6 ± 0.3***	0.3 ± 0.1***	0.2 ± 0.1***,&
Liver *Fth1* mRNA	1.0 ± 0.3	5.0 ± 1.4***	1.0 ± 0.6	3.1 ± 1.0***,&
Female	**Control (n = 8)**	**STA (n = 5)**	**Control (n = 8)**	**STA (n = 5)**
Liver Fe (µg/g)	166.0 ± 64.6	275.5 ± 118.0	1611.6 ± 313.4***	1606.5 ± 373.8***,&
Spleen Fe (µg/g)	1661.2 ± 682.7	2535.8 ± 890.4	2035.6 ± 776.9	2074.5 ± 827.1
Serum Fe (µg/dL)	164.3 ± 21.0	172.1 ± 48.0	273.1 ± 62.3*	243.6 ± 73.0
Transferrin Saturation (%)	48.2 ± 1.4	40.9 ± 5.3	86.8 ± 20.3*	72.9 ± 18.5&
Liver *Hamp* mRNA	1.0 ± 0.3	0.9 ± 0.3	0.4 ± 0.1***	0.6 ± 0.3
Liver *Fth1* mRNA	1.0 ± 0.1	0.8 ± 0.1	0.7 ± 0.1***	0.8 ± 0.2

Statistics were calculated using two-way ANOVA following Bonferroni's, multiple comparisons test. $*P < 0.05$, $***P < 0.001$ vs Control $Tfr2^{+/+}$, $^{\#}P < 0.01$ vs Control $Tfr2^{-/-}$, $^{\&}P < 0.05$ vs STA $Tfr2^{+/+}$.

Table S3

Quantification of pixel density of the proteome array spots in serum from $Tfr2^{+/+}$ and $Tfr2^{-/-}$ at day 10 after K/BxN serum transfer induced arthritis (STA).

Cytokines	$Tfr2^{+/+}$ STA (n = 4)	$Tfr2^{-/-}$ STA (n = 4)	P value
IL-7	10286.5 ± 1075.2	11984.5 ± 338.8	0.040
IL-16	10095.5 ± 1111.3	11803.9 ± 270.8	0.041
IL-17	11291.0 ± 1346.7	13512.4 ± 563.1	0.039
IL-27	10297.4 ± 1181.1	12701.2 ± 427.4	0.016
TNF-α	7981.9 ± 527.4	9778.4 ± 558.3	0.007
Chemokines			
CXCL1	6026.6 ± 861.8	8211.5 ± 370.5	0.012
CCL2	6386.5 ± 1010.1	8259.7 ± 4706	0.040

(continued on next page)

Table S3 (*continued*)

Cytokines	Tfr2$^{+/+}$ STA (n = 4)	Tfr2$^{-/-}$ STA (n = 4)	P value
CXCL11	9042.0 ± 1282.9	12302.4 ± 605.3	0.013
CCXL13	12724.9 ± 1108.2	16483.8 ± 1001.6	0.005
Inflammatory Proteins			
sCAM-1	18428.3 ± 1184.7	23874.2 ± 1103.8	0.001
G-CSF	9396.7 ± 617.3	12356.6 ± 571.5	0.001
M-CSF	13755.1 ± 1320.7	16805.8 ± 1467.4	0.037
TIMP-1	12081.9 ± 693.7	15652.2 ± 1327.9	0.006
TREM-1	10348.9 ± 725.7	12872.3 ± 706.0	0.005

Mean pixel density of each protein spot represents the average of four individual mice in each genotype. Statistics were calculated using Student's *t*-test.

Table S4

Hematological and iron parameters for *Tfr2$^{fl/fl}$; LysM-Cre* male and female mice subjected to K/BxN serum transfer induced arthritis (STA).

Male	Cre-		Cre+	
	Control (n = 8)	STA (n = 9)	Control (n = 7)	STA (n = 9)
Liver Fe (µg/g)	310.3 ± 94.0	323.3 ± 92.5	257.9 ± 127.2	262.1 ± 107.1
Spleen Fe (µg/g)	1766.9 ± 622.4	1768.8 ± 865.0	927.0 ± 567.5	1778.1 ± 811.8#
Serum Fe (µg/dL)	225.7 ± 48.3	188.4 ± 58.4	139.1 ± 66.4	129.3 ± 64.2
Transferrin Saturation (%)	74.3 ± 19.0	60.7 ± 21.6	45.4 ± 21.6	47.0 ± 19.9

Female	**Control (n = 8)**	**STA (n = 9)**	**Control (n = 8)**	**STA (n = 9)**
Liver Fe (µg/g)	376.1 ± 122.5	520.7 ± 83.9#	258.7 ± 123.4	590.2 ± 123.2**,#
Spleen Fe (µg/g)	2399.6 ± 881.0	3908.4 ± 741.1*,#	2190.9 ± 734.9	3424.6 ± 1174.9
Serum Fe (µg/dL)	219.6 ± 40.0	130.0 ± 36.1*	176.1 ± 66.6	138.7 ± 44.0
Transferrin Saturation (%)	72.5 ± 8.1	43.2 ± 11.6*	60.6 ± 18.4	43.4 ± 13.6*

Statistics were calculated using two-way ANOVA following Bonferroni's, multiple comparisons test. *$P < 0.05$, **$P < 0.01$ vs Control Cre-; #$P < 0.01$ vs Control Cre+.

Table S5

Quantification of pixel density of the proteome array spots in cell culture supernatant of bone marrow-derived macrophages (BMDM) isolated from *Tfr2$^{+/+}$* and *Tfr2$^{-/-}$* mice and stimulated with IFN-γ during 18h in the presence or absence of Ruxo.

Cytokines	Tfr2$^{+/+}$		Tfr2$^{-/-}$	
	IFN-γ	IFN-γ +Ruxo	IFN-γ	IFN-γ +Ruxo
IL-4	1780.0 ± 71.7	1786.5 ± 65.3	1965.0 ± 64.4&	1786.3 ± 33.7**
IL-6	1495.8 ± 38.3	1471.5 ± 16.3	1579.5 ± 29.2&	1456.5 ± 0.5***
IL-7	1908.05 ± 157.6	1879.5 ± 74.8	2150.8 ± 155.8&	1865.8 ± 50.2*
IL-16	2061.8 ± 326.8	1892.0 ± 16.3	2799.5 ± 249.3&	1889.8 ± 173.7**
IL-17	1832.0 ± 60.2	1888.8 ± 37.3	1861.8 ± 25.8	1794.0 ± 47.3**
IL-27	2361.3 ± 368.3	2153.5 ± 213.9	2968.9 ± 139.7&	1957.3 ± 58.2***
Chemokines				
CXCL1	1705.3 ± 75.1	1822.3 ± 158.6	1836.5 ± 54.5&	1723.5 ± 59.9
CCL3	1689.5 ± 68.3	1705.0 ± 58.5	1808.8 ± 46.7&	1682.3 ± 34.4**
CXCL9	5344.0 ± 944.7	3974.6 ± 1024.8	7308.6 ± 753.2&	3595.0 ± 555.8***
CXCL10				

Table S5 (*continued*)

Cytokines	Tfr2$^{+/+}$		Tfr2$^{-/-}$	
	IFN-γ	IFN-γ +Ruxo	IFN-γ	IFN-γ +Ruxo
	14781.4 ± 1036.6	14595.1 ± 2262.9	16876.1 ± 426.0&	16382.1 ± 64.4
CXCL11	2890.6 ± 958.0	2072.0 ± 156.8	4543.9 ± 204.9&	2181.8 ± 31.4***
CXCL13	1741.8 ± 56.1	1800.3 ± 107.8	1864.5 ± 52.1&	1852.8 ± 84.4
Inflammatory Proteins				
sCAM-1	5495.8 ± 1238.0	6590.1 ± 2144.5	7972.1 ± 1388.3&	4538.9 ± 508.0**
GM-CSF	1479.5 ± 31.5	1568.8 ± 49.3&	1537.0 ± 8.9&	1537.8 ± 9.1
M-CSF	2059.0 ± 192.8	2129.0 ± 150.2	2369.3 ± 152.3&	1944.3 ± 86.8**
TIMP-1	5989.0 ± 1011.6	6223.4 ± 1161.4	7560.3 ± 703.4&	5697.0 ± 1138.1
TREM-1	1684.3 ± 55.2	1713.8 ± 65.4	1766.3 ± 26.7&	1642.0 ± 21.3**
C5/C5a	1860.8 ± 80.6	1744.8 ± 50.5	2008.5 ± 72.8	1870.0 ± 46.0*

Mean pixel density of each protein spot represents the average of four individual samples in each genotype. Statistics were calculated using two-way ANOVA following Bonferroni's, multiple comparisons test. &$P < 0.05$ vs Tfr2$^{+/+}$+IFN-γ, *$P < 0.05$, **$P < 0.01$, ***$P < 0.001$ vs Tfr2$^{-/-}$ + IFN-γ.

Data availability

Data will be made available on request.

Appendix A. Supplementary data

Supplementary data to this article can be found online at https://doi.org/10.1016/j.redox.2023.102616.

References

[1] F.M. Brennan, I.B. McInnes, Evidence that cytokines play a role in rheumatoid arthritis, J. Clin. Invest. 118 (11) (2008) 3537–3545.

[2] I.B. McInnes, G. Schett, The pathogenesis of rheumatoid arthritis, N. Engl. J. Med. 365 (2011) 2205–2219.

[3] Q. Guo, Y. Wang, D. Xu, J. Nossent, N.J. Pavlos, J. Xu, Rheumatoid arthritis: pathological mechanisms and modern pharmacologic therapies, Bone Res 6 (2018) 15.

[4] R.M. Bennett, E.D. Williams, S.M. Lewis, P.J. Holt, Synovial iron deposition in rheumatoid arthritis, Arthritis Rheum. 16 (3) (1973) 298–304.

[5] J.F. Telfer, J.H. Brock, Proinflammatory cytokines increase iron uptake into human monocytes and synovial fibroblasts from patients with rheumatoid arthritis, Med. Sci. Mon. Int. Med. J. Exp. Clin. Res. 10 (4) (2004) BR91–B95.

[6] D.R. Blake, J. Lunec, M. Ahern, E.F. Ring, J. Bradfield, J.M. Gutteridge, Effect of intravenous iron dextran on rheumatoid synovitis, Ann. Rheum. Dis. 44 (3) (1985) 183–188.

[7] A.J. Dabbagh, D.R. Blake, C.J. Morris, Effect of iron complexes on adjuvant arthritis in rats, Ann. Rheum. Dis. 51 (4) (1992) 516–521.

[8] F.C. Breedveld, R. Dynesius-Trentham, M. de Sousa, D.E. Trentham, Collagen arthritis in the rat is initiated by CD4+ T cells and can be amplified by iron, Cell. Immunol. 121 (1) (1989) 1–12.

[9] D.R. Blake, N.D. Hall, P.A. Bacon, P.A. Dieppe, B. Halliwell, J.M. Gutteridge, Effect of a specific iron chelating agent on animal models of inflammation, Ann. Rheum. Dis. 42 (1) (1983) 89–93.

[10] M.U. Muckenthaler, S. Rivella, M.W. Hentze, B. Galy, A red carpet for iron metabolism, Cell 168 (3) (2017) 344–361.

[11] E. Nemeth, M.S. Tuttle, J. Powelson, M.B. Vaughn, A. Donovan, D.M. Ward, et al., Hepcidin regulates cellular iron efflux by binding to ferroportin and inducing its internalization, Science 306 (5704) (2004) 2090–2093.

[12] S. Aschemeyer, B. Qiao, D. Stefanova, E.V. Valore, A.C. Sek, T.A. Ruwe, et al., Structure-function analysis of ferroportin defines the binding site and an alternative mechanism of action of hepcidin, Blood 131 (8) (2018) 899–910.

[13] A. Pietrangelo, Hereditary hemochromatosis, Biochim. Biophys. Acta 1763 (7) (2006) 700–710.

[14] C.A. Worthen, C.A. Enns, The role of hepatic transferrin receptor 2 in the regulation of iron homeostasis in the body, Front. Pharmacol. 5 (2014) 34.

[15] G. Rishi, E.S. Secondes, D.F. Wallace, V.N. Subramaniam, Normal systemic iron homeostasis in mice with macrophage-specific deletion of transferrin receptor 2, Am. J. Physiol. Gastrointest. Liver Physiol. 310 (3) (2016) G171–G180.

[16] M. Rauner, U. Baschant, A. Roetto, R.M. Pellegrino, S. Rother, J. Salbach-Hirsch, et al., Transferrin receptor 2 controls bone mass and pathological bone formation via BMP and Wnt signalling, Nature Metabolism 1 (1) (2019) 111–124.

[17] R.M. Pellegrino, E. Boda, F. Montarolo, M. Boero, M. Mezzanotte, G. Saglio, et al., Transferrin receptor 2 dependent alterations of brain iron metabolism affect anxiety circuits in the mouse, Sci. Rep. 6 (2016), 30725.

[18] C. Camaschella, A. Roetto, A. Cali, M. De Gobbi, G. Garozzo, M. Carella, et al., The gene TFR2 is mutated in a new type of haemochromatosis mapping to 7q22, Nat. Genet. 25 (1) (2000) 14–15.

[19] H. Forejtnikova, M. Vieillevoye, Y. Zermati, M. Lambert, R.M. Pellegrino, S. Guihard, et al., Transferrin receptor 2 is a component of the erythropoietin receptor complex and is required for efficient erythropoiesis, Blood 116 (24) (2010) 5357–5367.

[20] A.D. Christensen, C. Haase, A.D. Cook, J.A. Hamilton, K/BxN serum-transfer arthritis as a model for human inflammatory arthritis, Front. Immunol. 7 (2016) 213.

[21] H.L. Wright, R.C. Bucknall, R.J. Moots, S.W. Edwards, Analysis of SF and plasma cytokines provides insights into the mechanisms of inflammatory arthritis and may predict response to therapy, Rheumatology (Oxford) 51 (3) (2012) 451–459.

[22] L.J.S. da Fonseca, V. Nunes-Souza, M.O.F. Goulart, L.A. Rabelo, Oxidative stress in rheumatoid arthritis: what the future might hold regarding novel biomarkers and add-on therapies, Oxid. Med. Cell. Longev. 2019 (2019), 7536805.

[23] D. Galaris, A. Barbouti, K. Pantopoulos, Iron homeostasis and oxidative stress: an intimate relationship, Biochim. Biophys. Acta Mol. Cell Res. 1866 (12) (2019), 118535.

[24] S. Li, H.Y. Tan, N. Wang, Z.J. Zhang, L. Lao, C.W. Wong, et al., The role of oxidative stress and antioxidants in liver diseases, Int. J. Mol. Sci. 16 (11) (2015) 26087–26124.

[25] G. Schett, E. Gravallese, Bone erosion in rheumatoid arthritis: mechanisms, diagnosis and treatment, Nat. Rev. Rheumatol. 8 (11) (2012) 656–664.

[26] H. Ji, K. Ohmura, U. Mahmood, D.M. Lee, F.M. Hofhuis, S.A. Boackle, et al., Arthritis critically dependent on innate immune system players, Immunity 16 (2) (2002) 157–168.

[27] B. Thapa, K. Lee, Metabolic influence on macrophage polarization and pathogenesis, BMB Rep 52 (6) (2019) 360–372.

[28] K. Schroder, P.J. Hertzog, T. Ravasi, D.A. Hume, Interferon-gamma: an overview of signals, mechanisms and functions, J. Leukoc. Biol. 75 (2) (2004) 163–189.

[29] E.M. Widdowson, R.A. McCance, Sexual differences in the storage and metabolism of iron, Biochem. J. 42 (4) (1948) 577–581.

[30] S.K. Das, V.B. Patel, R. Basu, W. Wang, J. DesAulniers, Z. Kassiri, et al., Females are protected from iron-overload cardiomyopathy independent of iron metabolism: key role of oxidative stress, J. Am. Heart Assoc. 6 (1) (2017).

[31] M. Wessling-Resnick, Iron homeostasis and the inflammatory response, Annu. Rev. Nutr. 30 (2010) 105–122.

[32] F.A. Khan, M.A. Fisher, R.A. Khakoo, Association of hemochromatosis with infectious diseases: expanding spectrum, Int. J. Infect. Dis. 11 (6) (2007) 482–487.

[33] C. Lehmann, S. Islam, S. Jarosch, J. Zhou, D. Hoskin, A. Greenshields, et al., The utility of iron chelators in the management of inflammatory disorders, Mediat. Inflamm. 2015 (2015), 516740.

[34] M. Cutolo, B. Seriolo, B. Villaggio, C. Pizzorni, C. Craviotto, A. Sulli, Androgens and estrogens modulate the immune and inflammatory responses in rheumatoid arthritis, Ann. N. Y. Acad. Sci. 966 (2002) 131–142.

[35] G. Zandman-Goddard, E. Peeva, Y. Shoenfeld, Gender and autoimmunity, Autoimmun. Rev. 6 (6) (2007) 366–372.

[36] B.T. Wipke, P.M. Allen, Essential role of neutrophils in the initiation and progression of a murine model of rheumatoid arthritis, J. Immunol. 167 (3) (2001) 1601–1608.

[37] E. Kolaczkowska, P. Kubes, Neutrophil recruitment and function in health and inflammation, Nat. Rev. Immunol. 13 (3) (2013) 159–175.

[38] C. Renassia, S. Louis, S. Cuvellier, N. Boussetta, J.C. Deschemin, D. Borderie, et al., Neutrophils from hereditary hemochromatosis patients are protected from iron excess and are primed, Blood Adv 4 (16) (2020) 3853–3863.

[39] P. Italiani, D. Boraschi, From monocytes to M1/M2 macrophages: phenotypical vs. Functional differentiation, Front. Immunol. 5 (2014) 514.

[40] G. Weiss, D. Fuchs, A. Hausen, G. Reibnegger, E.R. Werner, G. Werner-Felmayer, et al., Iron modulates interferon-gamma effects in the human myelomonocytic cell line THP-1, Exp. Hematol. 20 (5) (1992) 605–610.

[41] G. Weiss, G. Werner-Felmayer, E.R. Werner, K. Grunewald, H. Wachter, M. W. Hentze, Iron regulates nitric oxide synthase activity by controlling nuclear transcription, J. Exp. Med. 180 (3) (1994) 969–976.

[42] D.F. Wallace, L. Summerville, P.E. Lusby, V.N. Subramaniam, First phenotypic description of transferrin receptor 2 knockout mouse, and the role of hepcidin, Gut 54 (7) (2005) 980–986.

[43] E. Wyart, M.Y. Hsu, R. Sartori, E. Mina, V. Rausch, E.S. Pierobon, et al., Iron supplementation is sufficient to rescue skeletal muscle mass and function in cancer cachexia, EMBO Rep. 23 (4) (2022), e53746.

[44] C.V. Ramana, M.P. Gil, Y. Han, R.M. Ransohoff, R.D. Schreiber, G.R. Stark, Stat1-independent regulation of gene expression in response to IFN-gamma, Proc. Natl. Acad. Sci. U. S. A. 98 (12) (2001) 6674–6679.

[45] L. Valenti, M. Varenna, A.L. Fracanzani, V. Rossi, S. Fargion, L. Sinigaglia, Association between iron overload and osteoporosis in patients with hereditary hemochromatosis, Osteoporos. Int. 20 (4) (2009) 549–555.

[46] M.G. Ledesma-Colunga, H. Weidner, M. Vujic Spasic, L.C. Hofbauer, U. Baschant, M. Rauner, Shaping the bone through iron and iron-related proteins, Semin. Hematol. 58 (3) (2021) 188–200.

[47] P. Guggenbuhl, P. Fergelot, M. Doyard, H. Libouban, M.P. Roth, Y. Gallois, et al., Bone status in a mouse model of genetic hemochromatosis, Osteoporos. Int. 22 (8) (2011) 2313–2319.

[48] M.G. Ledesma-Colunga, U. Baschant, I.A.K. Fiedler, B. Busse, L.C. Hofbauer, M. U. Muckenthaler, et al., Disruption of the hepcidin/ferroportin regulatory circuitry causes low axial bone mass in mice, Bone 137 (2020), 115400.

[49] G.S. Shen, Q. Yang, J.L. Jian, G.Y. Zhao, L.L. Liu, X. Wang, et al., Hepcidin 1 knockout mice display defects in bone microarchitecture and changes of bone formation markers, Calcif. Tissue Int. 94 (6) (2014) 632–639.

[50] K.A. Ishii, T. Fumoto, K. Iwai, S. Takeshita, M. Ito, N. Shimohata, et al., Coordination of PGC-1 beta and iron uptake in mitochondrial biogenesis and osteoclast activation, Nat. Med. 15 (3) (2009) 259–266.